VOL. 11, NO. 3, FEBRUARY 2016 ISSN 1819-6608
ARPN Journal of Engineering and Applied Sciences

www.arpnjournals.com

A NEW TECHNIQUE FOR FAULT DETECTION IN INDUCTION MOTOR

A. Elamathi[1] and K. Preetha[2]
[1]Power Electronics and Drives, DSEC, Perambalur, Tamil Nadu, India
[2]Department of Electrical and Electronics Engineering, DSEC, Perambalur, Tamil Nadu, India

ABSTRACT

Fault tolerance is gaining interest as a means to increase the reliability and availability of distributed energy system. In this project presents a new technique for fault detection in vector controlled induction motor (IM) drive. The proposed current estimation uses estimation uses d- and q-axes currents and is independent of the switching states of the three-leg inverter. While the technique introduces a new concept of vector rotation to generate potential estimates of the currents, speed is estimated by one of the available model reference adaptive system (MRAS) based formulations. The objective of the controller was to control the current that supply into the induction motor. The proposed method is extensively simulated in simulated in MATLAB/SIMULINK.

Keywords: current estimation, fault detection, induction motor (IM) drive, model reference adaptive system, speed estimation.

1. INTRODUCTION

Induction motor (IM) drives are extensively used in industry due to their cost effectiveness, ruggedness and low maintenance requirements. Field-oriented-controlled or vector controlled drive has become an industry standard for high performance applications. Speed, current, and/or voltage sensors are usually required in vector controlled drives. Rotor speed information is necessary for speed-controlled system. The fast current controller operates in the inner current loop and a slower speed controller stays in the outer speed loop to generate the corresponding reference currents for the current controllers. Efforts are put to reduce the number of sensors by signal estimation/processing. The source of failure may bedue to the machine (such as stator interturn faults, broken bar in the rotor, etc.), converter (i.e., failure of the switching devices), or maloperation of sensors. In vector-controlled drives, speed and current (and/or voltage) sensors are usually required. The maloperation of current and speed sensors (due tonoise, dc-offset and open circuit, etc.) is not uncommon in the industrial environment, and any industrial drive system needsto be prepared to take care of such contingencies. Therefore, sensor fault-tolerant control is an extremely important area of investigation for IM drives. Fault-tolerant control in IM has opted for one of the two approaches. In the first approach, when a fault is detected, the system switches to an alternative form of controller (typically from a closed-loop to open-loop control), whereas in the second technique, the loop is closed by the corresponding signal fromthe estimator/observer. A thorough definition of relevant terminology has been given the following:

1) Fault: unpermitted deviation of at least one characteristic property or parameter of a system from its acceptable/ usual/standard condition;

2) Residual: fault indicator, based on deviation between measurements and model-equation-based computations;

3) Fault detection: determination of faults present in a system and time of detection;

4) Fault isolation: determination of type, location, and time of detection of a fault; follows fault detection. This definition should be amended with the term;

5) Reconfiguration: rearrangement of the control structure of a system that enables continued operation in spite of a fault.

If a fault is detected, the current signals from the current sensors are ignored and are replaced by estimated current signals computed using the parameters of the machine. The proposed technique demands more design efforts and is computationally intensive, which makes their real-time implementation difficult. Fault-tolerant drive for multiple sensor failure is also proposed. However, this is at the cost of an additional sensor at the dc link. In, a programmable logic controller (PLC) based protection and monitoring method for three-phase IM is present.

Now a day the controllers that had been widely used to overcome this problem are from adaptive and passive controller such as Field Oriented Control (FOC), Direct Torque Control (DTC), Proportional Integral Derivatives (PID), Fuzzy, Neural Network, Sliding Mode Control (SMC), and Hysteresis. The current regulation has played important role in current controlled pulse-width-modulated (PWM) inverter which widely applied in high performance AC drives. Beside that there were several parameters that must be considered, such as the current control technique to the induction motor. For this case the Hysteresis Current Control Technique was being used.

This project proposed a new fault detection technique to make the IM drive fault tolerant against current and speed sensor failures. The compensation for current and speed needs a method of estimation. A new concept of vector rotation to identify the faulty current sensor is introduced. A logic-based detection mechanism in the α–β reference frame is proposed to make the drive fault tolerant against current sensor failures. The speed estimation is carried out by modifying a recently proposed model reference adaptive system (MRAS)-based technique.

2. PROPOSED SPEED ESTIMATION ALGORITHM

The speed is estimated using the concept of MRAS, where a reference and an adjustable model

VOL. 11, NO. 3, FEBRUARY 2016 ISSN 1819-6608
ARPN Journal of Engineering and Applied Sciences

compute a certain system variable (in literature this is known as functional candidate). The system variable computed by the reference model does not depend on the quantity to be estimated, whereas the adjustable model depends directly or indirectly on the estimated quantity.

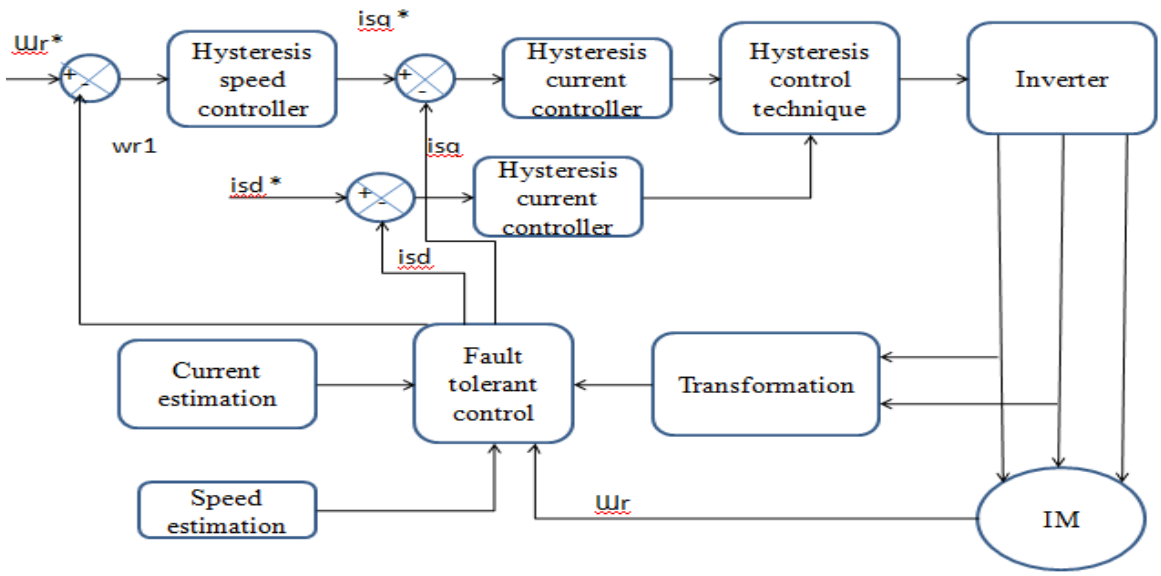

Figure-1. Block diagram.

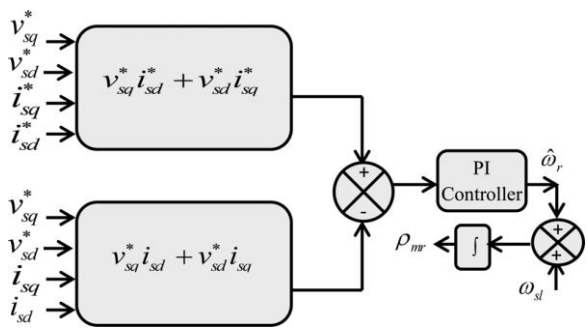

Figure-2. Structure of speed estimation.

Like P and Q, here a fictitious (i.e., has no physical existence) quantity, termed as$X(X = _v*s\times_is)$ is considered as the functional candidate. The quantity X in reference model (Xr) is computed using the reference values of voltages and currents. The same value of X in adjustable model (Xa) is computed with the help of reference values of voltages and actual currents. The actual values of d- and q-axis currents are obtained by transforming two-phase currents (i.e., $is\alpha$ and $\hat{}is\beta$) with the help of vector rotator (which, in turn, depends on speed). The signal $\hat{}is\beta$ is obtained from the current estimation algorithm. The structure of the speed estimation algorithm is shown in Figure-2. The reference model computes Xr using the controller generated command signals and hence does not require the information of rotor speed. On the contrary, (3) shows that the expression of Xa involves rotor speed, as ρmr is computed using (4).

$$Xr = v*sq\ i*sd + v*sd\ i*sq \quad (1)$$

$$Xa = v*sq\ isa\ e{-}j\rho m\ r + v*sdis\beta\ e{-}j\rho mr \quad (3)$$

$$\rho mr = \int \omega edt \quad (4)$$

where

$$\omega e = \hat{}\omega r + \omega sl\ .$$

Model Reference Adaptive System (MRAS) is one of the famous speed observers usually used for sensorless induction motor drives. It is one of many promising techniques employed in adaptive control. Among various types of adaptive system configuration, MRAS is important since it leads to relatively easy-to-implement systems with high speed of adaptation for a wide range of applications. One of the most noted advantages of this type of adaptive system is its high speed of adaptation.

VOL. 11, NO. 3, FEBRUARY 2016 ISSN 1819-6608
ARPN Journal of Engineering and Applied Sciences

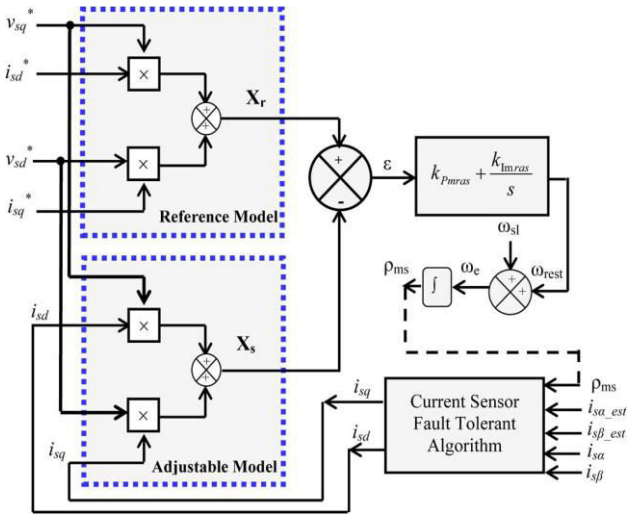

Figure-3. MRAS structure for speed estimation.

This is due to the fact that a measurement of the difference between the outputs of the reference model and adjustable model is obtained directly by the comparison of the states (or outputs) of the reference model with those of the adjustable system. The block ‘‘reference model’’ represents demanded dynamics of actual control loop. The block ‘‘adjustable model’’ has the same structure as the reference one, but with adjustable parameters instead of the unknown ones. The MRAS speed estimation structure consists basically of a reference model, adjustable model and an adaptive mechanism. The reference model, which is independent of the rotor speed, calculates the state variable, x, from the terminal voltage and current. The adjustable model, which is dependent on the rotor speed, estimates the state variable, xˆ. The error ε between calculated and estimated state variables is then used to drive an adaptation mechanism which generates the estimated speed, ˆωr, for the adjustable model. The main advantages of MRAS algorithms are they robustness, fast convergence and small computation time. Selection of adaptive mechanism gains is a compromise between achieving fast response and high robustness against noise and disturbances affecting the system.

2. CURRENT ESTIMATION

This section deals with the estimation of current and also the fault detection. That the transformations from three phase to two-phase quantities require the individual orientation of the axes with respect to each other. Following the standard procedure, first, it is assumed that the a-phase (of the three phase system) and α-phase (of the two-phase system) are along the same axes (see Figure-4). The corresponding relation between a–b and α–β variables is shown by (4). A close inspection of reveals that, if a-phase sensor is defective, then both α- and β-phase measurements will be wrong. However, if the b-phase sensor is defective, the corresponding current of the α-phase will remain correct, while the current in the β-phase will be wrong.

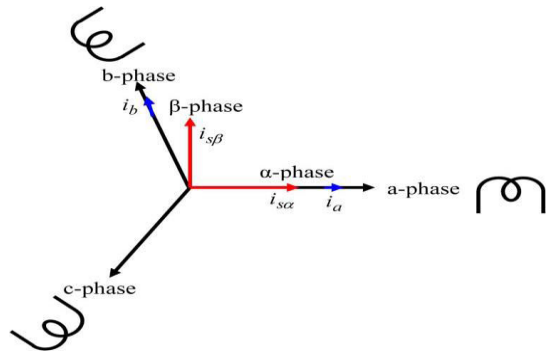

Figure-4. Axes transformation showing α phase along a phase.

$$\begin{bmatrix} i_{s\alpha} \\ i_{s\beta} \end{bmatrix} = \begin{bmatrix} \frac{3}{2} & 0 \\ \frac{\sqrt{3}}{2} & \sqrt{3} \end{bmatrix} \begin{bmatrix} i_a \\ i_b \end{bmatrix}$$

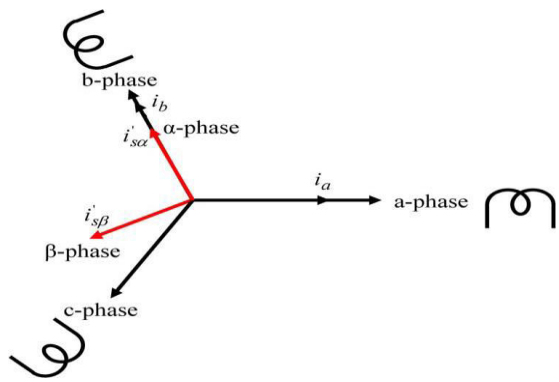

Figure-5. Axes transformation showing α phase along b phase.

On the other hand, a unique feature is extracted if the α–βphase are rotated by 120◦. This is shown in Figure-5. The corresponding relation for the conversion of three-phase to two phase current is shown in (5).

$$\begin{bmatrix} i'_{s\alpha} \\ i'_{s\beta} \end{bmatrix} = \begin{bmatrix} 0 & \frac{3}{2} \\ -\sqrt{3} & -\frac{\sqrt{3}}{2} \end{bmatrix} \begin{bmatrix} i_a \\ i_b \end{bmatrix}$$

Est

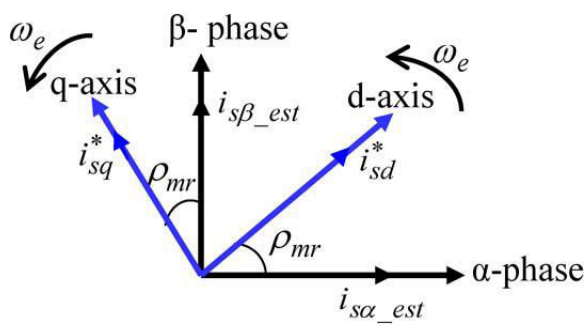

Figure-6. Estimation of current when α phase along a phase.

Using the actual measurement of a- and b- phase currents and the corresponding reference-magnitude of the same in the (d, q) rotating reference frame, eight estimates of currents in the α–β reference frame are thus possible. These are $is\alpha$, $is\beta$,$i\_s\alpha$, $i\_s\beta$, $is\alpha\_est$, $is\beta\_est$, $i\_s\alpha\_est$, and $i\_s\beta\_est$, where $is\alpha$,$is\beta$, $is\alpha\_est$, are $is\beta\_est$ are the corresponding variables whenα-phase is along a-phase and $i\_s\alpha$, $i\_s\beta$, $i\_s\alpha\_est$, and $i\_s\beta\_est$ arethe corresponding variables when α-phase is along b-phase.

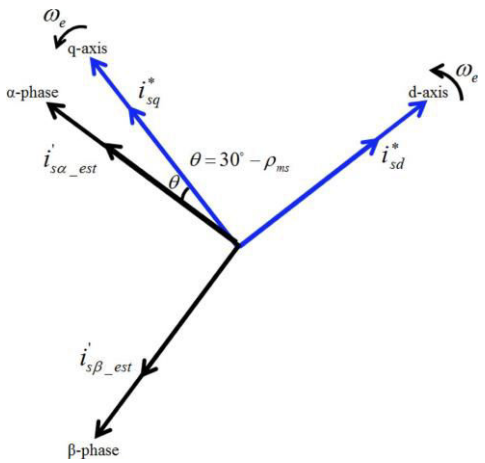

Figure-7. Estimation of current when α phase along b phase.

3. HYSTERESIS CONTROLLER

A. Concept of hysteresis control

Hysteresis control (also called "bang-bang" or "tolerance band" control) utilizes a defined upper and lower limit based on a reference waveform. The load current is monitored and maintained within certain limits of that reference waveform.

a) The hysteresis band

The hysteresis band defines an acceptable error in the load current based around a reference ac waveform, *i*ref . By simply applying a positive and negative dc offset, $I_h$to *i*ref, the hysteresis band ,Δ_h is established. More precisely, Δ_h is defined as the difference between the upper and lower boundaries,

$$\Delta_h = i_{\text{ref}} + I_h - (i_{\text{ref}} - I_h) = 2I_h.$$

A hysteresis control circuit monitors the load current and appropriately switches the transistors to ensure the load current remains within the hysteresis band. In the control circuit, i_{ref} is represented as a voltage proportional to the desired output current, out *i* out, with a conversion factor of 1 A/V. (In fact, all currents are converted to voltage signals at1 A/V for ease of use by the control circuit.) Figure-8 shows a 2-Apeak, 60-Hz wave form, *i* ref, with 0.2 A (Δ_h = 0.4 A).

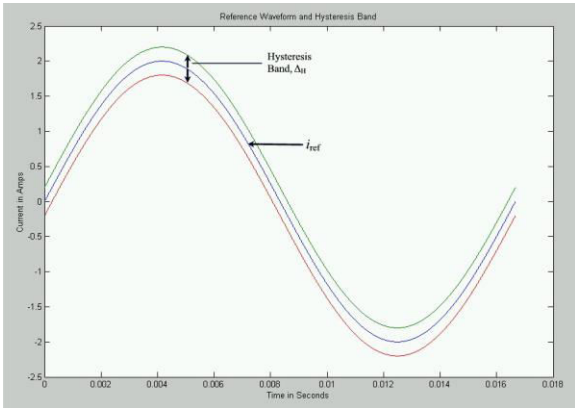

Figure-8. Hysteresis band.

The hysteresis band in above Figure appears wider at the upper and lower peaks than at the zero crossing; however, the band is measured vertically at a specific time instant and is a constant 0.4 A throughout the cycle.

The circuitry required to define the hysteresis band uses summing and difference amplifiers, as shown in Figure-9.

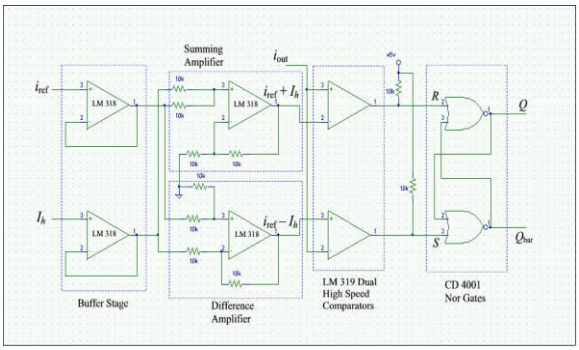

Figure-9. Hysteresis control circuit.

b) Feedback

Measurement of the load current is accomplished via a Hall effect device, which provides electrical isolation between the load current and control electronics. A Hall effect device senses the load current and produces its own output current proportional to the load current. The current from the Hall effect sensor is passed through a measuring (burdening) resistor to produce a voltage that corresponds to the measured current. Thus, by appropriate choice of the measuring resistor, the feedback signal can be scaled making it possible to monitor and control a very large load current with a small feedback signal, *i*out. As shown in Figure-9, *i* out is fed into a pair of comparators to determine whether or not it has reached one of the boundaries of the hysteresis band. When *i* outreaches a boundary, the comparators force the *RS* flip-flop to change state and switch the transistors" on" or "off" as appropriate.

VOL. 11, NO. 3, FEBRUARY 2016 ISSN 1819-6608
ARPN Journal of Engineering and Applied Sciences

www.arpnjournals.com

c) Gating signals

Gating a transistor means turning it "on" and should not be confused with the digital logic term "gate", as in "nor gate". The *RS* flip-flop provides the gating signals for the transistors. Figure 9 neither shows the RS flip-flop implemented with two "nor" gates and contains the function table for an *RS* flip-flop. Even though the flip-flop has the indeterminate state $R \llcorner\lrcorner S \llcorner 1$, this state is impossible; the only way that $R \llcorner\lrcorner S \llcorner 1$ can occur is if the measured feedback signal, *i* out is both above and below the hysteresis band at the same instant in time. Should the flip-flop, for some reason, be in the indeterminate state at start-up, the control circuitry will immediately force it to exit that state and go to one of the other three states. The output of the flip-flop is used to gate the transistors; *Q* gates the upper and *Q*bar gates the lower.

5. SIMULATION RESULTS

This section deals with the simulation results of proposed system. The proposed fault detection system is experimentally validated with the matlab/ simulink

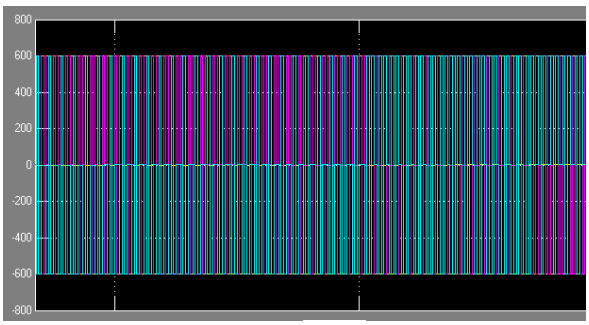

Time, s

Figure-10. Voltage waveform.

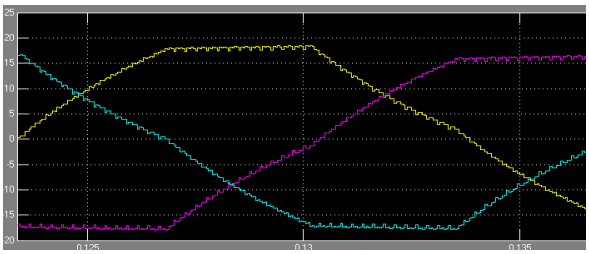

Time, s

Figure-11. Current waveforms.

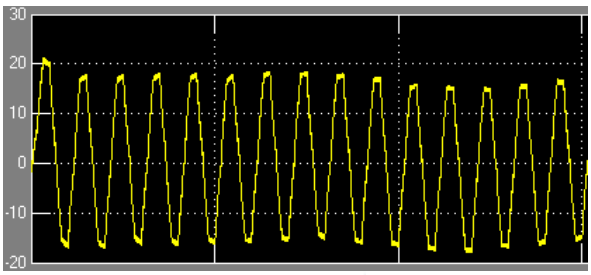

Time, s

Figure-12. Stator a phase current.

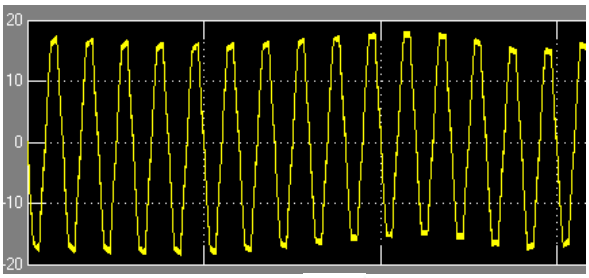

Time, s

Figure-13. Stator b phase current.

6. CONCLUSIONS

A new technique for fault detection in vector controlled Induction motor is presented in this project. New techniques to estimate speed and current are utilized for the implementation. While the current estimation is based on the reference currents in synchronously rotating reference frame and the vector rotator, the speed estimation exploits a different form of X-MRAS, Both the techniques to not involve stator resistance. Hence the proposed controller works very well at low speed. The proposed concept is extensively simulated in MATLAB/Simulink.

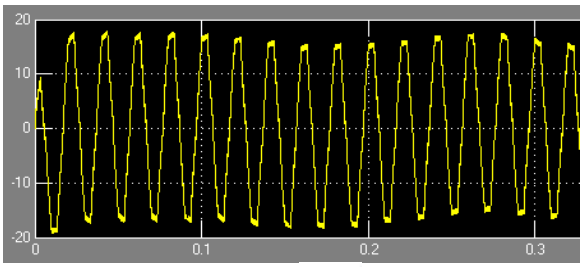

Time, s

Figure-14. Stator c phase current.

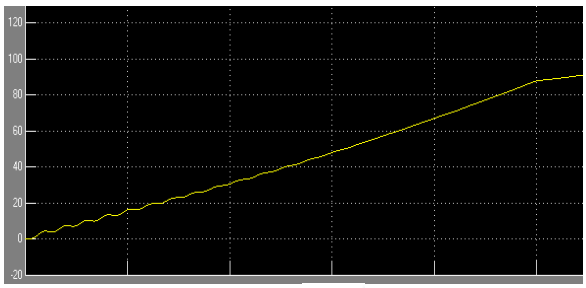

Time, s

Figure-15. Rotor speed.

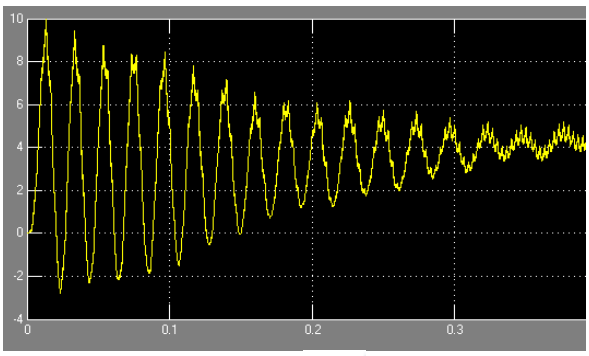

Time, s

Figure-16. Torque.

List of symbols

$V_{s\alpha}$, $V_{S\beta}$	α and β components of the stator voltage vector.
$i_{s\alpha}$, $i_{S\beta}$	α and β phase currents when α-phase is along a- phase.
$i^1_{s\alpha}$, $i^1_{s\beta}$	α and β phase currents when α-phase is along b- phase.
$i_{s\alpha\_est}$, $i_{S\beta\_est}$	Estimated value of α and β phase currents when α-phase is along b-phase.
$i^1_{s\alpha\_est}$, $i^1_{s\beta\_est}$	Estimated value of α and β phase currents when α-phase is along b-phase.
$i^*_{s\alpha}$, $i^*_{s\alpha\beta}$	Reference value of d- and q-axes currents.
ω_r^*, ω_r, ω_{rest}	Reference, actual,and estimated rotor speed.
ω_{sl}	Slip speed.
R_s	Stator resistance.
L_S, L_r	Self inductance at the stator and the rotor side.
L_m	Magnetizing inductance.
i_a, i_b	a and b- phase currents.
ρ_{ms}	Rotor flux angle with the α-phase.

REFERENCES

[1] Y. Gritli *et al*. 2013. Advanced diagnosis of electrical faults in wound-rotorinduction machines. IEEE Trans. Ind. Electron. vol. 60, no. 9, pp. 4012–4024, September.

[2] S. Toma, L. Capocchi, and G. A. Capolino. 2013. Wound rotor induction generator inter-turn short-circuits diagnosis using a new digital neural network. IEEE Trans. Ind. Electron., vol. 60, no. 9, pp. 4043-4052, September.

[3] M. P. Sanchez *et al*. Application of the Teager-Kaiser energy operatorto the fault diagnosis of induction motors. IEEE Trans. Energy Convers. vol. 28, no. 4, pp. 1036–1044, December.

[4] S. H. Kia, H. Henao, and G. A. Capolino. Gear tooth surface damage fault detection using induction machine electrical signature analysis. In: Proc. SDEMPED, Valencia, Spain, pp. 358-364.

[5] A. Bernieri, G. Betta, A. Pietrosanto, and C. Sansone. 1995. A neural network approach to instrument fault detection and isolation. IEEE Trans. Instrum. Meas., vol. 44, no. 3, pp. 747–750, June.

[6] G. Betta, C. Liguori, and A. Pietrosanto. 1998. An advanced neural-network based instrument fault detection and isolation scheme. IEEE Trans. Instrum. Meas. vol. 47, no. 2, pp. 507–512, April.

[7] F. Zidani, M. E. H. Benbouzid, D. Diallo, and A. Benchaib. 2003. Active fault tolerant control of induction motor drives in EV and HEV against sensor failures using a fuzzy decision system. In: Proc. IEEE IEMDC, vol. 2, pp. 677-683.

[8] K. S. Lee and J. S. Ryu. 2003. Instrument fault detection and compensation scheme for direct torque controlled induction motor drives. Proc. Inst. Elect. Eng.-Control Theory Appl., vol. 150, no. 4, pp. 376–382, July.

[9] D. Diallo, M. E. H. Benbouzid, and A. Makouf. 2004. A fault-tolerant control architecture for induction motor drives in automotive applications. IEEE Trans. Veh. Technol. vol. 53, no. 6, pp. 1847–1855, November.

[10] H. Wang, S. Pekarak, and B. Fahimi. 2006. Multilayer control of an induction motor drive: A strategic step for automotive applications. IEEE Trans. Power Electron. vol. 21, no. 3, pp. 676-686, May.

[11] M. E. H. Benbouzid, D. Diallo, and M. Zeraoulia, 2007. Advanced fault tolerant control of induction-motor drives for EV/HEV traction application: From conventional to modern and intelligent control techniques. IEEE Trans. Veh. Technol. vol. 56, no. 2, pp. 519–528, March.

[12] F. Zidani, D. Diallo, M. E. H. Benbouzid, and E. Berthelot. 2007. Diagnosis of speed sensor failure in induction motor drive. In: Proc. IEEE IEMDC. vol. 2, pp. 1680–1684.

[13] D. U. C. Delgado, D. R. E. Trejo, and E. Palacios. 2008. Fault-tolerant control in variable speed drives: A survey. IET Electr. Power Appl. vol. 2, no. 2, pp. 121–134, March.

[14] R. Bayindir, I. Sefa, I. Colak, and A. Bektas. 2008. Fault detection and protection of induction motors using sensors. IEEE Trans. Energy Convers. vol. 23, no. 3, pp. 734–741, September.

[15] M. E. Romero, M. M. Seron, and J. A. D. Dona. 2010. Sensor fault-tolerant vector control of induction motors. IET Control Theory Appl. vol. 4, no. 9, pp. 1707–1724, September.

[16] T. A. Najafabadi, F. R. Salmasi, and P. J. Maralani. 2011. Detection and isolation of speed-, dc-link voltage-, and current-sensor faults based on an adaptive observer in induction-motor drives. IEEE Trans. Ind. Electron. vol. 58, no. 5, pp. 1662-1672, May.

[17] F. R. Salmasi and T. A. Najafabadi. 2011. An adaptive observer with onlinerotor and stator resistance estimation for induction motors with one phase current sensor. IEEE Trans. Energy Convers, vol. 26, no. 3, pp. 959-966, September.

[18] H. Berriri, M. W. Naouar, and I. S. Belkhodja. 2012. Easy and fast sensor fault detection and isolation algorithm for electrical drives. IEEE Trans. Power Electron. vol. 27, no. 2, pp. 490–499, February.

[19] H. Li, A. Monti, and F. Ponci. 2012. A fuzzy-based sensor validation strategy for ac motor drives. IEEE Trans. Ind. Informat. vol. 8, no. 4, pp. 839–848, November.

[20] B. Tabbache, N. Rizoug, M. E. H. Benbouzid, and A. Kheloui. 2013. A control reconfiguration strategy for post-sensor FTC in induction motor based EVs. IEEE Trans. Veh. Technol. vol. 62, no. 3, pp. 965–971, March.

[21] B. Tabbache, M. E. H. Benbouzid, A. Kheloui, and J. M. Bourgeot. 2013. Virtual-sensor-based maximum-likelihood voting approach for fault tolerant control of electric vehicle powertrains. IEEE Trans. Veh. Technol. vol. 62, no. 3, pp. 1075-1083, March.

[22] X. Zhang *et al.* 2013. Sensor fault detection, isolation and system reconfiguration based on extended Kalman filter for induction motor drives. IETElect. Power Appl. vol. 7, no. 7, pp. 607-617, August.

[23] M. Boukhnifer, A. Raisemche, D. Diallo, and C. Larouci. Fault tolerant control to mechanical sensor failures for induction motor drive: A comparative study of voting algorithms. In: Proc. IEEE IECON, Vienna, Austria. pp. 2851-2856.